

Polyol-responsive pseudopolyrotaxanes based on phenylboronic acid-modified polyethylene glycol and cyclodextrins

Yu Kojima, Tomoyuki Okano, Tomohiro Seki, Misato Namiki, Yuya Egawa,\* Ryotaro Miki, Kazuhiko Juni and Toshinobu Seki

*Faculty of Pharmaceutical Sciences, Josai University, 1-1 Keyakidai, Sakado, Saitama 350-0295, Japan*

\* [yegawa@josai.ac.jp](mailto:yegawa@josai.ac.jp)

Tel +81-49-271-7686

Fax +81-49-271-7714

### **Acknowledgements**

This work was supported by Grants-in-Aid for Scientific Research of the Japan Society for the Promotion of Science (KAKENHI, JSPS) Grant Number 25860027.

### **Abstract**

Phenylboronic acid (PBA), which reacts with polyols to form cyclic esters, was attached to the amino terminal of polyethylene glycol (PEG) *via* amide bonds. PBA-PEG was used to prepare pseudopolyrotaxanes (pPRXs) by combining it with cyclodextrins (CyDs). In the case of  $\alpha$ -CyD, a single stranded pPRX formed that disintegrated in the presence of catechol (CA), D-fructose (Fru), and D-glucose (Glc). The order of response was CA > Fru > Glc, which corresponds with the affinities between the PBA moiety and the polyols. In contrast, a pPRX using  $\gamma$ -CyD, which has a double-stranded structure, showed sugar-induced disintegration but did not show a response to CA. We explained these apparently curious responses of the pPRXs using a mechanism based on the penetrability of the polyol-bound PBA toward the cavities of the CyDs. The pPRXs, which are a class of molecular machine, show two selectivities; one is derived from polyol selectivity, and the other is based on the penetrability for CyDs.

### **Keywords**

pseudopolyrotaxane; cyclodextrin; boronic acid; drug delivery; stimuli-responsive material

## Introduction

Cyclodextrins (CyDs) are cyclic oligosaccharides that are widely used in pharmaceutical fields. The inclusion of drug molecules within CyDs is a well-known strategy to improve the solubility and stability of drugs [1, 2]. In recent years, more sophisticated supramolecular structures based on CyDs have attracted much attention for use in drug delivery systems (DDS), tissue engineering, and regenerative medicines [3, 4]. In the field of supramolecular chemistry, terms of rotaxane, polyrotaxane, and pseudopolyrotaxanes (pPRX) have been used [5]. Rotaxane is a type of mechanically interlocked supramolecular structure, which is composed of a dumbbell-shaped molecule and a cyclic molecule. The cyclic molecule covers the bar of the dumbbell and the terminal bulky parts of the dumbbell work as a stopper to prevent the cyclic molecule from falling off. Polyrotaxane structure contains several cyclic molecules trapped by a long dumbbell molecule. The word “pseudo” in the term “pPRX” refers to the absence of terminal bulky groups, thereby allowing many cyclic molecules to slip through the bar molecule.

pPRXs composed of polymer and CyD have been the subject of intensive study. For example, covering poly( $\epsilon$ -caprolactone) with  $\alpha$ -CyD afforded certain favorable characteristics to bio-scaffolds [4]. In the pharmaceutical area, the dynamic and reversible change between the formation and destruction of pPRX would be suitable for forming molecular machines for DDS. In particular, pPRXs in which many CyDs are threaded by linear polyethylene glycol (PEG), have been intensively studied [6]. PEG is biocompatible and can escape the reticuloendothelial system [7]. Some PEGylated drugs are currently on the market. CyDs are also biocompatible; therefore, pPRXs based on PEG and CyD may be suitable as drug delivery systems. Higashi *et al.* created a novel strategy to prepare sustained release systems for PEGylated proteins using pPRXs [8–10]. A pPRX composed of PEGylated insulin and CyDs disintegrated gradually, functioning as a long-acting insulin delivery system.

These studies encouraged us to develop a new drug delivery system that exploits the disintegration properties of pPRXs. Recently, we proposed the concept of pPRXs using phenylboronic acid (PBA) as a sugar recognition motif. The pPRXs containing PBA showed sugar-induced disintegration [11–13]. PBA is a Lewis acid that coordinates with  $\text{OH}^-$  to form a boronate. The boronate form can interact with the diol moiety of a polyol to form a cyclic ester; the reaction is rapid and reversible, and a state of equilibrium can therefore be achieved depending on the concentration of the polyol [14]. Utilizing this rapid and reversible reaction of PBA, analytical chemists have attempted to create chemical sensors to monitor blood D-glucose (Glc) levels [15–18]. Furthermore, some pharmaceutical scientists have attempted to incorporate PBA as a sugar recognition motif into insulin delivery systems in which the interaction between PBA and Glc is expected to function as a trigger for insulin release [19–22]. A technology which releases insulin only at necessary times and in the needed amounts is urgently required because self-injection treatments of insulin have some drawbacks, such as risk of hypoglycemia [23].

PBA derivatives tend to interact strongly with catechol (CA) and D-fructose (Fru). According to

published data, the binding constants of PBA at pH 7.4 to CA, Fru, and Glc are 830, 160, and 4.6 M<sup>-1</sup>, respectively [24]. First, we should note that PBA and CyDs do not form cyclic esters, although CyDs are sugars. PBA usually interacts with the furanose forms of sugars [25, 26]. In contrast, CyDs are composed of glucopyranose units; thus, the steric arrangement of their hydroxyl groups is unsuitable for the formation of cyclic esters with PBA. Some reports have shown that CyDs act as host molecules for PBA to form inclusion complexes rather than as sugars to form cyclic esters with PBA [27–30].

In our previous communication [13], PBA was attached to the hydroxyl groups of PEG through carboxyl ester bonds, and the resulting compound was applied to form a pPRX using  $\gamma$ -CyD. We attempted to obtain a pPRX using  $\alpha$ -CyD; however, we were not successful because  $\alpha$ -CyD facilitated hydrolysis of the carboxylic ester bonds between PBA and PEG during the pPRX formation process. The pPRX containing  $\gamma$ -CyD showed sugar-induced disintegration, and we proposed a mechanism to explain this. However, the mechanism was supported by only one case, the pPRX containing  $\gamma$ -CyD; further empirical examples are needed to validate this proposed mechanism.

In this study, we prepared chemically stable PBA-modified PEG through the formation of amide bonds (PBA-PEG) and used it to prepare pPRXs by combining it with  $\alpha$ -CyD and  $\gamma$ -CyD (Fig. 1). We observed the responses of the pPRXs to polyols and attempted to apply our proposed mechanism to explain these responses. In this report, we show a further example of a pPRX using  $\alpha$ -CyD and PBA-PEG to demonstrate the validity of our proposed mechanism.

## Experimental

### Materials

$\alpha$ -CyD and  $\gamma$ -CyD were purchased from Junsei Chemical Co., Ltd. (Tokyo, Japan). Amino-PEG (H<sub>2</sub>N-(CH<sub>2</sub>)<sub>3</sub>O-PEG-(CH<sub>2</sub>)<sub>3</sub>-NH<sub>2</sub>; SUNBRIGHT® DE-020PA) was purchased from NOF Corporation (Tokyo, Japan). According to the manufacturer, the average molecular weight was 2121, and the terminal activation rate was 89.9%. *p*-Carboxyphenylboronic acid and 4-(2-hydroxyethyl)-1-piperazineethanesulfonic acid (HEPES) were obtained from Sigma-Aldrich Japan (Tokyo, Japan). 1-Ethyl-3-(3-dimethylaminopropyl)carbodiimide (EDC) was purchased from Tokyo Chemical Industry Co., Ltd. (Tokyo, Japan). All other chemicals were of reagent grade and were used as received.

### Apparatus

Differential scanning calorimetry (DSC) was conducted using a Thermo Plus 2 series instrument (Rigaku Corporation, Tokyo, Japan). The sample was heated in an aluminum pan under nitrogen atmosphere at a heating rate of 5 K/min. Powder X-ray diffraction (XRD) patterns were measured using a Mini FlexII

instrument (Rigaku Corporation) under the following conditions: 30 kV CuK $\alpha$  radiation and 15 mA diffraction with a scanning speed of 4°/min and a measurement range of  $2\theta = 2^\circ$  to  $39^\circ$ .  $^1\text{H}$  NMR spectra were measured with a Varian 400-MR spectrometer (Agilent Technologies, Santa Clara, CA, USA). Turbidity was monitored with a V-530 UV-vis spectrometer (JASCO Corporation, Tokyo, Japan) using the absorbance at 700 nm.

### Synthesis of PBA-PEG

*p*-Carboxyphenylboronic acid (761 mg, 4.59 mmol), EDC (1.06 g, 5.53 mmol), and pyridine (682  $\mu\text{L}$ ) were added to a solvent mixture of dichloromethane (DCM) dried with  $\text{MgSO}_4$  (100 mL) and anhydrous dimethylsulfoxide (DMSO, 25 mL) at  $0^\circ\text{C}$ . The mixture was stirred under nitrogen atmosphere for 15 min. Then, amino-PEG (531 mg, 0.250 mmol) was added; the resulting suspension was stirred at room temperature under nitrogen atmosphere. After three days, the DCM was evaporated. The resulting DMSO solution was mixed with 300 mL of slightly acidic water and adjusted to pH 3.6 by adding 1.0 M HCl. The solution was filtered to remove the insoluble matter, and the filtrate was dialyzed against water using a dialysis tube (MWCO 1000). The resulting solution was lyophilized, and PBA-PEG was obtained (290 mg, 48.0%).  $^1\text{H}$  NMR (400 MHz,  $\text{DMSO-}d_6$ )  $\delta$  8.19–8.14 (s, 3.0H, BOH), 7.87–7.71 (s, 6.8H, phenyl-H), 3.51–3.47 (m, 180H, PEG) (Fig. S1). The manufacturer reported that average molecular weight was 2121; therefore, the repeat number of ethylene glycol was 45, and the integration of the signal was set to 180H. If the terminal activation rate was 100%, the proton-derived phenyl-H would be 8H. The result of 6.8H indicates that 85% of the terminals were modified with PBA; also, almost all the amino groups were converted to amide bonds because the manufacturer of the amino-PEG indicated that 89.9% of the terminal amino groups were activated.

### Preparation of pPRXs

PBA-PEG (13.3 mg, 5.50  $\mu\text{mol}$ ) and  $\alpha$ -CyD (120 mg, 123  $\mu\text{mol}$ ) were dissolved in water (1.00 mL), and the solution was maintained at room temperature. After three days, the resulting precipitate of molecular necklaces was filtered and dried under reduced pressure (39.4 mg). The obtained pPRX was dissolved in  $\text{DMSO-}d_6$  and measured by  $^1\text{H}$  NMR spectroscopy (Fig. S2).

In a similar manner, PBA-PEG (33.9 mg, 14.0  $\mu\text{mol}$ ) and  $\gamma$ -CyD (200 mg, 154  $\mu\text{mol}$ ) were mixed in water (1.00 mL), and a precipitate was obtained (199 mg).

### Turbidity measurements

A buffer solution (20 mM HEPES, pH 7.4, 2.0 mL) was stirred in an absorption spectrometer cell at  $37^\circ\text{C}$ .

pPRX( $\alpha$ -CyD/PBA-PEG) (100 to 125 mg) was suspended in the stirred buffer solution. The turbidity was recorded by the absorbance at 700 nm. The turbidity was allowed to reach a constant absorbance value of approximately 2; a small amount of polyol solution (Glc, Fru, CA, 1.00 M) was added at 10-min intervals to the suspension to increase the polyol concentration.

In a similar manner, pPRX( $\gamma$ -CyD/PBA-PEG) (40 to 43 mg) was added to a cell until an absorption value of approximately 2 was reached, and stock solutions of polyol were added to the suspension.

## Results and Discussion

### *Preparation of the pPRXs*

We successfully obtained chemically stable PBA-PEG by condensing amino-PEG and 4-carboxyphenylboronic acid with EDC. The  $^1\text{H}$  NMR spectrum of PBA-PEG shows a signal at 3.5 ppm that is derived from the ethylene glycol units. Assuming that the ethylene glycol proton integration of amino-PEG was 180H, the modification ratio of the PBA moiety was calculated to be 85%. Almost all the amino groups were modified with PBA because the terminal activation ratio of amino-PEG was reported by the manufacturer to be 90%.

The obtained PBA-PEG and CyDs were dissolved in water, and white precipitates were obtained for both  $\alpha$ -CyD and  $\gamma$ -CyD. The precipitates were analyzed by DSC and XRD to confirm that they were pPRXs.

In the DSC thermograph of PBA-PEG alone, an endothermic peak was observed at 43 °C, corresponding to the melting point of PBA-PEG (Fig. 2a). In the thermograph of the precipitate obtained from the solution of  $\alpha$ -CyD and PBA-PEG, the endothermic peak completely disappeared (Fig. 2c), indicating the absence of the crystal structure of PBA-PEG by the effect of  $\alpha$ -CyD. Therefore, the result indicated the formation of pPRX composed of  $\alpha$ -CyD and PBA-PEG. Similarly, there was no endothermic peak in Fig. 2e, which suggests the formation of pPRX composed of  $\gamma$ -CyD and PBA-PEG.

Fig. 3 shows the XRD patterns of the obtained precipitates. The pattern of the precipitate obtained from  $\alpha$ -CyD and PBA-PEG (Fig. 3c) was very similar to that of a hexagonal columnar channel structure of a pPRX containing  $\alpha$ -CyD and native PEG [31, 32]. The peaks in the pattern were converted to the observed  $d$ -spacing ( $d_{\text{obs}}$ ) using equation 1. On the basis of an assumption that the peak at  $2\theta = 7.48^\circ$  was derived from  $hkl$  (200) of the hexagonal system, the two-dimensional unit cells were calculated as  $a = b = 27.27 \text{ \AA}$ . Using this value of the unit cells and equation 2, the  $d$ -spacing values were calculated ( $d_{\text{cal}}$ ), which agreed well with  $d_{\text{obs}}$  values (Table 1). This agreement supports the formation of a hexagonal crystal system of pPRX( $\alpha$ -CyD/PBA-PEG).

The pattern of the precipitate obtained from  $\gamma$ -CyD and PBA-PEG (Fig. 3e) resembled that of a tetragonal columnar channel structure of a pPRX containing  $\gamma$ -CyD and native PEG [12, 32]. On the basis of an assumption that the peak at  $2\theta = 7.46^\circ$  was derived from  $hkl$  (200) of the tetragonal system, the

two-dimensional unit cells were calculated as  $a = b = 23.68 \text{ \AA}$ . From this value and equation 3,  $d_{\text{cal}}$  values were obtained, which agreed well with the  $d_{\text{obs}}$  values, thereby supporting the formation of a tetragonal crystal system of pPRX( $\gamma$ -CyD/PBA-PEG) (Table 2). These results of the DSC and XRD analyses support the formation of pPRXs.

$$2d\sin\theta = \lambda \quad \dots(1)$$

$$d_{hkl} = \frac{1}{\sqrt{\frac{4}{3} \frac{h^2 + hk + k^2}{a^2} + \frac{l^2}{c^2}}} \quad \dots (2)$$

$$d_{hkl} = \frac{1}{\sqrt{\frac{h^2 + k^2}{a^2} + \frac{l^2}{c^2}}} \quad \dots (3)$$

To confirm the stoichiometry of the components of the pPRXs, they were dissolved in DMSO- $d_6$ , and the solutions were analyzed by  $^1\text{H}$  NMR spectroscopy. The spectrum of pPRX( $\alpha$ -CyD/PBA-PEG) shows that H-1 of  $\alpha$ -CyD was observed at 4.8 ppm (Fig. S2). When the integration of H-1 of  $\alpha$ -CyD (4.8 ppm) was set to 6.00, the integration value of PEG (3.5 ppm) was 12.6. From this result, we calculated the stoichiometric ratio of the ethylene glycol unit and  $\alpha$ -CyD was 3.2:1.0. Assuming the formation of a single-stranded pPRX in which two ethylene glycol units are included in one CyD molecule [33], the coverage of pPRX( $\alpha$ -CyD/PBA-PEG) was calculated to be 63%. The coverage was low compared to that of a pPRX composed of  $\alpha$ -CyD and native PEG [34]. We believe that the low coverage is due to the bulkiness of the PBA terminal. Kato *et al.* also reported that a bulky terminal resulted in low coverage [35].

More importantly, the  $^1\text{H}$  NMR spectrum showed that the terminal PBA moiety (approximately 7.8 ppm in Fig. S2) was retained during the pPRX formation process due to the stability of PBA-PEG, although this attempt was unsuccessful in our previous communication [13].

In the case of pPRX( $\gamma$ -CyD/PBA-PEG), the integration of PEG was 18.5 when the H-1 of CyD was set to 8.00 (Fig. S3). From this result, the stoichiometric ratio between the ethylene glycol unit and  $\gamma$ -CyD was calculated to be 4.6:1.0, and the coverage was calculated to be 87% based on the formation of a double-stranded pPRX containing  $\gamma$ -CyD [36].

The results of the DSC, XRD, and  $^1\text{H}$  NMR analyses demonstrate that pPRX( $\alpha$ -CyD/PBA-PEG) and pPRX( $\gamma$ -CyD/PBA-PEG) were successfully obtained.

#### *Polyol responses of the pPRXs*

The polyol responses of the obtained pPRXs containing PBA-PEG were studied by turbidity

measurements (Fig. 4). pPRX( $\alpha$ -CyD/PBA-PEG) was suspended in a buffer solution (2.0 mL, 20 mM HEPES buffer, pH 7.4, 37 °C). After the turbidity became constant, a small amount of stock solution of polyol was added to the suspension to increase the polyol concentration in the measurement cell. The turbidity due to solid state pPRX( $\alpha$ -CyD/PBA-PEG) significantly decreased with increasing CA concentration (Fig. 4), which indicates that the pPRX disintegrated and the components were dissolved. All three polyols used in this study, CA, Fru, and Glc, induced disintegration. The response of pPRX( $\alpha$ -CyD/PBA-PBA) increased depending on the strength of the affinity between PBA and the polyol.

In the case of pPRX( $\gamma$ -CyD/PBA-PEG), Glc and Fru induced disintegration; however, CA had a negligible effect on the turbidity despite its high affinity for PBA (Fig. 4b). The results using  $\gamma$ -CyD were similar to that in a previous report [13]. In this study, we observed opposite responses of the pPRXs to CA; this information is valuable to understand the mechanism of the operating principle of the pPRXs.

Incidentally, it is noted that the percentage of turbidity values in Fig. 4 is not equal to that of the remaining the solid state pPRX. We investigated the relation between the turbidity and the weight of solid state pPRX, which showed that it was not a linear one (Fig. S4). Therefore, the turbidity value in Fig. 4 should be used only as a guide for the dissociation of pPRXs.

#### *Mechanism of sugar response*

To explain all these results, we employed our proposed mechanism, which consists of four equilibriums (Fig. 5) [13]. The first equilibrium, Eq. 1 in Fig. 5, shows the formation and deformation of the pPRXs. In other words, Eq.1 is a solubility equilibrium. We assumed that the pPRX is only in the solid state, and disintegration of the pPRX indicates that each component has dissolved. In a suspension, some amounts of CyD and PBA-PEG are dissolved. Eqs. 2, 3, and 4 should be considered when the sugars Fru and Glc are added to the suspension. Eqs. 2 and 3 are the interactions between the PBA moiety and the sugars. Eq. 4 is the formation and deformation of the complex of sugar-bound PBA-PEG and CyDs.

We considered that the size relationship between the polyols and the cavities of the CyDs may have an important effect on the responses of the pPRXs. Fig. 6 shows the space-filling models of the CyDs and the terminal structure of PBA-PEG. The diameter of the narrower side of  $\alpha$ -CyD is 0.47 nm [1]. The diameter of the benzene ring is 0.50 nm, which is slightly larger than the cavity of  $\alpha$ -CyD; therefore, the benzene ring can pass through the cavity of  $\alpha$ -CyD. In fact, the successful formation of the pPRXs demonstrates that the PBA terminal can pass through both CyDs. Fig. 6(e) shows the Fru-bound PBA structure proposed by Norrild and Eggert, in which the 2,3,6-hydroxyl groups of  $\beta$ -D-fructofuranose are connected with boron atoms [25]. Glc-bound PBA appears to be similar in size. Comparing Fig. 6(a) and (e), it is difficult for Fru-bound PBA to pass through  $\alpha$ -CyD. In the case of  $\gamma$ -CyD, one Fru-bound PBA molecule may pass through the  $\gamma$ -CyD cavity when it is vacant. However,  $\gamma$ -CyD must include two PEG

chains to form the pPRX. It is impossible for the two bulky terminals to pass through the cavity at the same time, and it is also difficult for the bulky terminal to pass through a  $\gamma$ -CyD cavity in which one PEG chain has already been included. From these aspects of the size relationship, we have concluded that the binding of a sugar decreases its permeability toward the CyD cavity.

There are two possible effects of the sugars on the pPRX. If the sugars attach to the solid state pPRX, through Eq. 2 in Fig. 5, the bulky terminal will act as a stopper, resulting in the formation of the polyrotaxane structure; this would stabilize the solid state species and increase its amount. In contrast, if the sugar attaches to dissolved PBA-PEG, through Eq. 3 in Fig. 5, the bulky terminal will block the interaction with CyDs, resulting in an increase in the amount of dissolved state.

In the abovementioned turbidity experiments, both Fru and Glc decreased the turbidity, *i.e.*, the amount of solid state decreased and the amount of dissolved state increased. This result indicates that the major role of the sugar-bound terminal is to block the reformation of the pPRX, but not to function as a stopper for the polyrotaxane. To explain the responses of the pPRXs, Eq. 3 is more important than Eq. 2 in our proposed mechanism. In the case of the sugars, Eq. 4 does not exist because the bulky blocker inhibits the cavities of  $\alpha$ -CyD and  $\gamma$ -CyD.

#### *Mechanism of CA response*

The binding of CA to the terminal PBA induced a slight change in the diameter for threading; however, the CA-bound PBA terminal has a non-planar structure because the boron atom exists in a  $sp^3$  hybridized tetragonal form, as shown in Fig. 6(d). The steric bulk of CA-bound PBA made it difficult to thread  $\alpha$ -CyD. Therefore, CA acts as a blocker to prevent the threading of  $\alpha$ -CyD (Fig. 7a), which is the reason for the observed disintegration of pPRX( $\alpha$ -CyD/PBA-PEG).

As shown in Fig. 6, the CA-PBA complex (Fig. 6d) is small enough to pass through the empty cavity of  $\gamma$ -CyD (Fig. 6b). Since CA bound PBA-PEG can pass through the  $\gamma$ -CyD cavity (Eq. 4 in Fig. 7b), CA does not act as a blocker for threading  $\gamma$ -CyD or as a stopper for dethreading  $\gamma$ -CyD; thus, this pPRX did not show a response to CA. In our proposed mechanism, Eq. 4 actually exists when CA,  $\gamma$ -CyD, and PBA-PEG are used because CA-PBA-PEG can pass through the  $\gamma$ -CyD cavity. Harada reported a similar case [36].  $\gamma$ -CyD formed pPRXs with PEG modified with relatively bulky stoppers, such as 2-naphtylacetyl groups and 3,5-dinitrobenzoyl groups; however,  $\alpha$ -CyD could not form a pPRX with PEG modified with bulky terminals.

#### **4. Conclusions**

We have prepared chemically stable PBA-PEG and used it to prepare pPRXs using  $\alpha$ -CyD and  $\gamma$ -CyD. Fru and Glc induced disintegration in the pPRXs containing both  $\alpha$ -CyD and  $\gamma$ -CyD. In contrast, CA

induced disintegration of the pPRX containing  $\alpha$ -CyD but showed negligible effects on the pPRX containing  $\gamma$ -CyD. This seemingly contradictory response of the pPRXs to polyols can be explained using our proposed mechanism.

We have concluded that the mechanism of the pPRX response is as follows. The polyol binds to the PBA moiety and increases its bulk. When the bulky terminal becomes too large to pass through the CyD cavity, the pPRX disintegrates because the bulky terminal acts as a blocker for the reformation of the pPRX. Glc and Fru act as blockers for the pPRXs containing both  $\alpha$ -CyD and  $\gamma$ -CyD. CA also acts as a blocker for the pPRX containing  $\alpha$ -CyD; however, CA does not affect the pPRX containing  $\gamma$ -CyD because the CA-bound terminal can pass through the cavity of  $\gamma$ -CyD.

These pPRXs are expected to find applications for sugar-induced insulin delivery systems, such as pPRX(CyD/PBA-PEG-modified insulin). In human bodies, the post-meal glucose level should be less than 10 mM [23]. Thereby, an ideal insulin-release system works at a level above 10 mM. However, the current system of pPRX does not have enough sensitivity for Glc. In the field of chemical sensors, some dimeric PBA sensors have been reported that strongly bind the Glc and selectively to work in blood Glc level [16]. For future studies, introducing the concept of dimeric PBA will be an attractive subject.

From the view point of supramolecular chemistry, the pPRXs show two selectivities; one is due to the polyol selectivity of PBA, and the other is based on the penetrability for CyDs. The operating principle of this pPRX is quite new which may pave the way for a new type of molecular machine.

## References

1. Szejtli, J.: Introduction and general overview of cyclodextrin chemistry. *Chem. Rev.* 98, 1743–1753 (1998).
2. Kurkov, S. V., Loftsson, T.: Cyclodextrins. *Int. J. Pharm.* 453, 167–180 (2013).
3. Antoniuk, I., Amiel, C.: Cyclodextrin-mediated hierarchical self-assembly and Its potential in drug delivery applications. *J. Pharm. Sci.* 105, 2570–2588 (2016).
4. Narayanan, G., Aguda, R., Hartman, M., Chung, C.C., Boy, R., Gupta, B.S., Tonelli, A.E.: Fabrication and characterization of poly( $\epsilon$ -caprolactone)/ $\alpha$ -cyclodextrin pseudorotaxane nanofibers. *Biomacromolecules.* 17, 271–279 (2016).
5. Wenz, G., Han, B.H., Müller, A.: Cyclodextrin rotaxanes and polyrotaxanes. *Chem. Rev.* 106, 782–817 (2006).
6. Harada, A., Hashizume, A., Yamaguchi, H., Takashima, Y.: Polymeric rotaxanes. *Chem. Rev.* 109, 5974–6023 (2009).
7. Veronese, F.M., Pasut, G.: PEGylation, successful approach to drug delivery. *Drug Discov. Today.* 10, 1451–1458 (2005).

8. Higashi, T., Hirayama, F., Arima, H., Uekama, K.: Polypseudorotaxanes of pegylated insulin with cyclodextrins: application to sustained release system. *Bioorg. Med. Chem. Lett.* 17, 1871–1874 (2007).
9. Higashi, T., Hirayama, F., Yamashita, S., Misumi, S., Arima, H., Uekama, K.: Slow-release system of pegylated lysozyme utilizing formation of polypseudorotaxanes with cyclodextrins. *Int. J. Pharm.* 374, 26–32 (2009).
10. Higashi, T., Hirayama, F., Misumi, S., Motoyama, K., Arima, H., Uekama, K.: Polypseudorotaxane formation of randomly-pegylated insulin with cyclodextrins: slow release and resistance to enzymatic degradation. *Chem. Pharm. Bull.* 57, 541–544 (2009).
11. Seki, T., Abe, K., Nakamura, K., Egawa, Y., Miki, R., Juni, K., Seki, T.: Sugar-responsive pseudopolyrotaxanes and their application in sugar-induced release of PEGylated insulin. *J. Incl. Phenom. Macrocycl. Chem.* 82, 417–424 (2015).
12. Seki, T., Abe, K., Egawa, Y., Miki, R., Juni, K., Seki, T.: A Pseudopolyrotaxane for Glucose-Responsive Insulin Release: The Effect of Binding Ability and Spatial Arrangement of Phenylboronic Acid Group. *Molecular Pharmaceutics.* 13, 3807–3815 (2016).
13. Seki, T., Namiki, M., Egawa, Y., Miki, R., Juni, K., Seki, T.: Sugar-responsive pseudopolyrotaxane composed of phenylboronic acid-modified polyethylene glycol and  $\gamma$ -cyclodextrin. *Materials.* 8, 1341–1349 (2015).
14. James, T.D.: Self and directed assembly: people and molecules. *Beilstein J. Org. Chem.* 12, 391–405 (2016).
15. Fossey, J.S., D’Hooge, F., van den Elsen, J.M.H., Pereira Morais, M.P., Pascu, S.I., Bull, S.D., Marken, F., Jenkins, A.T.A., Jiang, Y.-B., James, T.D.: The development of boronic acids as sensors and separation tools. *Chem. Rec.* 12, 464–478 (2012).
16. Wu, X., Li, Z., Chen, X.-X., Fossey, J.S., James, T.D., Jiang, Y.-B.: Selective sensing of saccharides using simple boronic acids and their aggregates. *Chem. Soc. Rev.* 42, 8032–8048 (2013).
17. Egawa, Y., Seki, T., Takahashi, S., Anzai, J.: Electrochemical and optical sugar sensors based on phenylboronic acid and its derivatives. *Mater. Sci. Eng. C.* 31, 1257–1264 (2011).
18. Egawa, Y., Miki, R., Seki, T.: Colorimetric sugar sensing using boronic acid-substituted azobenzenes. *Materials.* 7, 1201–1220 (2014).
19. Matsumoto, A., Yoshida, R., Kataoka, K.: Glucose-responsive polymer gel bearing phenylborate derivative as a glucose-sensing moiety operating at the physiological pH. *Biomacromolecules.* 5, 1038–1045 (2004).
20. De Geest, B.G., Jonas, A.M., Demeester, J., De Smedt, S.C.: Glucose-responsive polyelectrolyte capsules. *Langmuir.* 22, 5070–5074 (2006).

21. Watahiki, R., Sato, K., Suwa, K., Niina, S., Egawa, Y., Seki, T., Anzai, J.: Multilayer films composed of phenylboronic acid-modified dendrimers sensitive to glucose under physiological conditions. *J. Mater. Chem. B*. 2, 5809–5817 (2014).
22. Suwa, K., Nagasaka, M., Niina, S., Egawa, Y., Seki, T., Anzai, J.: Sugar response of layer-by-layer films composed of poly(vinyl alcohol) and poly(amidoamine) dendrimer bearing 4-carboxyphenylboronic acid. *Colloid Polym. Sci.* 293, 1043–1048 (2015).
23. American Diabetes Association: Standards of medical care in diabetes-2016 abridged for primary care providers. *Clin. Diabetes*. 34, 3–21 (2016).
24. Springsteen, G., Wang, B.: A detailed examination of boronic acid-diol complexation. *Tetrahedron*. 58, 5291–5300 (2002).
25. Norrild, J.C., Eggert, H.: Boronic acids as fructose sensors. Structure determination of the complexes involved using  $^1J_{cc}$  coupling constants. *J. Chem. Soc., Perkin Trans. 2*. 2583–2588 (1996).
26. Pan, X., Yang, X., Lowe, C.R.: Evidence for a cross-linking mechanism underlying glucose-induced contraction of phenylboronate hydrogel. *J. Mol. Reconit.* 21, 205–209 (2008).
27. Ozawa, R., Hayashita, T., Matsui, T., Nakayama, C., Yamauchi, A., Suzuki, I.: Effects of cyclodextrins and saccharides on dual fluorescence of *N,N*-dimethyl-4-aminophenylboronic acid in water. *J. Incl. Phenom. Macrocycl. Chem.* 60, 253–261 (2007).
28. Suzuki, I., Yamauchi, A., Sakashita, Y., Hirose, K., Miura, T., Hayashita, T.: Fluorescence response mechanism of D-glucose selectivity for supramolecular probes composed of phenylboronic-acid-modified beta-cyclodextrin and styrylpyridinium dyes. *Anal. Sci.* 23, 1167–1171 (2007).
29. Nakamura, K., Seki, T., Egawa, Y., Miki, R., Oda, Y., Yamanoi, T., Seki, T.: Sugar-sensitive supramolecular structures based on phenylboronic acid modified cyclodextrins. *Chem. Pharm. Bull.* 61, 1188–1191 (2013).
30. Wu, X., Lin, L.-R., Huang, Y.-J., Li, Z., Jiang, Y.-B.: A 2 : 2 stilbeneboronic acid- $\gamma$ -cyclodextrin fluorescent ensemble highly selective for glucose in aqueous solutions. *Chem. Commun.* 48, 4362–4364 (2012).
31. Topchieva, I.N., Tonelli, A.E., Panova, I.G., Matuchina, E. V, Kalashnikov, F. a, Gerasimov, V.I., Rusa, C.C., Rusa, M., Hunt, M. a: Two-phase channel structures based on alpha-cyclodextrin-polyethylene glycol inclusion complexes. *Langmuir*. 20, 9036–43 (2004).
32. Higashi, T., Tajima, A., Ohshita, N., Hirotsu, T., Hashim, I.I.A., Motoyama, K., Koyama, S., Iibuchi, R., Mieda, S., Handa, K., Kimoto, T., Arima, H.: Design and evaluation of the highly concentrated human IgG formulation using cyclodextrin polypseudorotaxane hydrogels. *AAPS PharmSciTech.* 16, 1290–1298 (2015).

33. Harada, A., Kamachi, M.: Complex formation between poly(ethylene glycol) and  $\alpha$ -cyclodextrin. *Macromolecules*. 23, 2821–2823 (1990).
34. Harada, A., Li, J., Kamachi, M.: Formation of inclusion complexes of monodisperse oligo(ethylene glycol)s with  $\alpha$ -cyclodextrin. *Macromolecules*. 27, 4538–4543 (1994).
35. Kato, K., Okabe, Y., Okazumi, Y., Ito, K.: A significant impact of host–guest stoichiometry on the extensibility of polyrotaxane gels. *Chem. Commun.* 51, 16180–16183 (2015).
36. Harada, A., Li, J., Kamachi, M.: Double-stranded inclusion complexes of cyclodextrin threaded on poly (ethylene glycol). *Nature*. 370, 126–128 (1994).
37. Chaplin M.: Cyclodextrins (Jmol), <http://www1.lsbu.ac.uk/water/cyclo.html>.

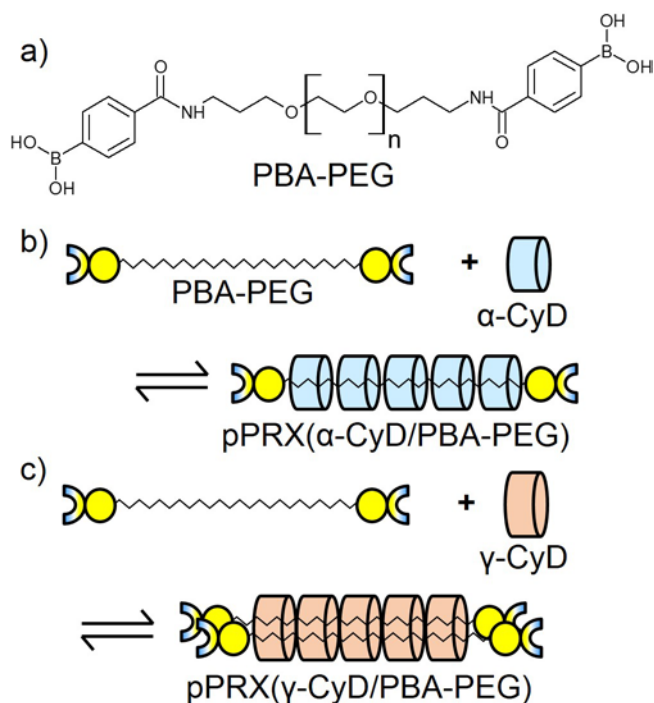


**Fig. 1** Chemical structure of PBA-PEG and schematics of the formation of the pPRXs. (a) PBA-PEG, (b) pPRX( $\alpha$ -CyD/PBA-PEG), (c) pPRX( $\gamma$ -CyD/PBA-PEG)

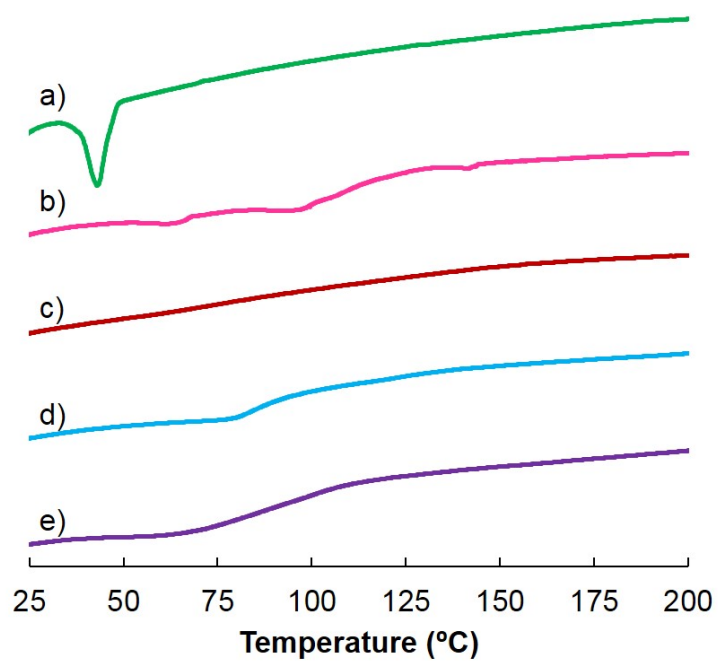


**Fig. 2** DSC thermograms: (a) PBA-PEG, (b)  $\alpha$ -CyD, (c) pPRX( $\alpha$ -CyD/PBA-PEG), (d)  $\gamma$ -CyD, (e) pPRX( $\gamma$ -CyD/PBA-PEG)

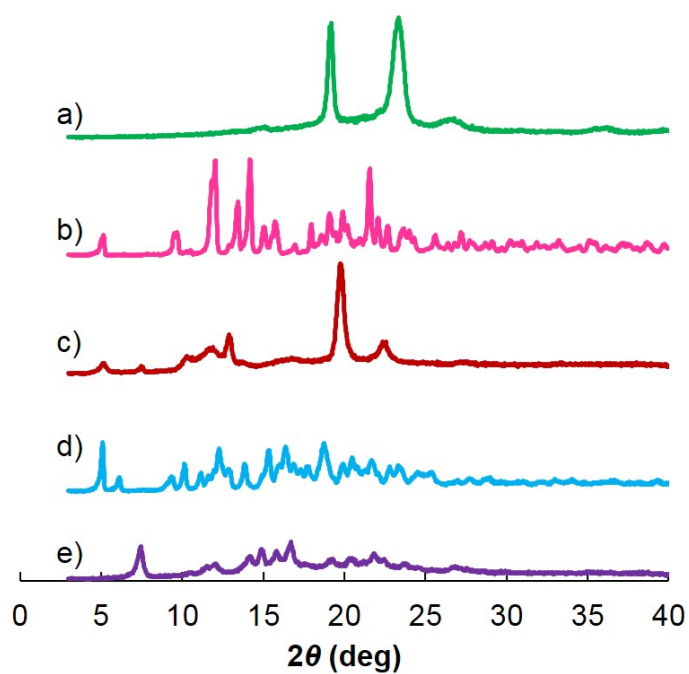


**Fig. 3** XRD patterns: (a) PBA-PEG, (b)  $\alpha$ -CyD, (c) pPRX( $\alpha$ -CyD/PBA-PEG), (d)  $\gamma$ -CyD, (e) pPRX( $\gamma$ -CyD/PBA-PEG)

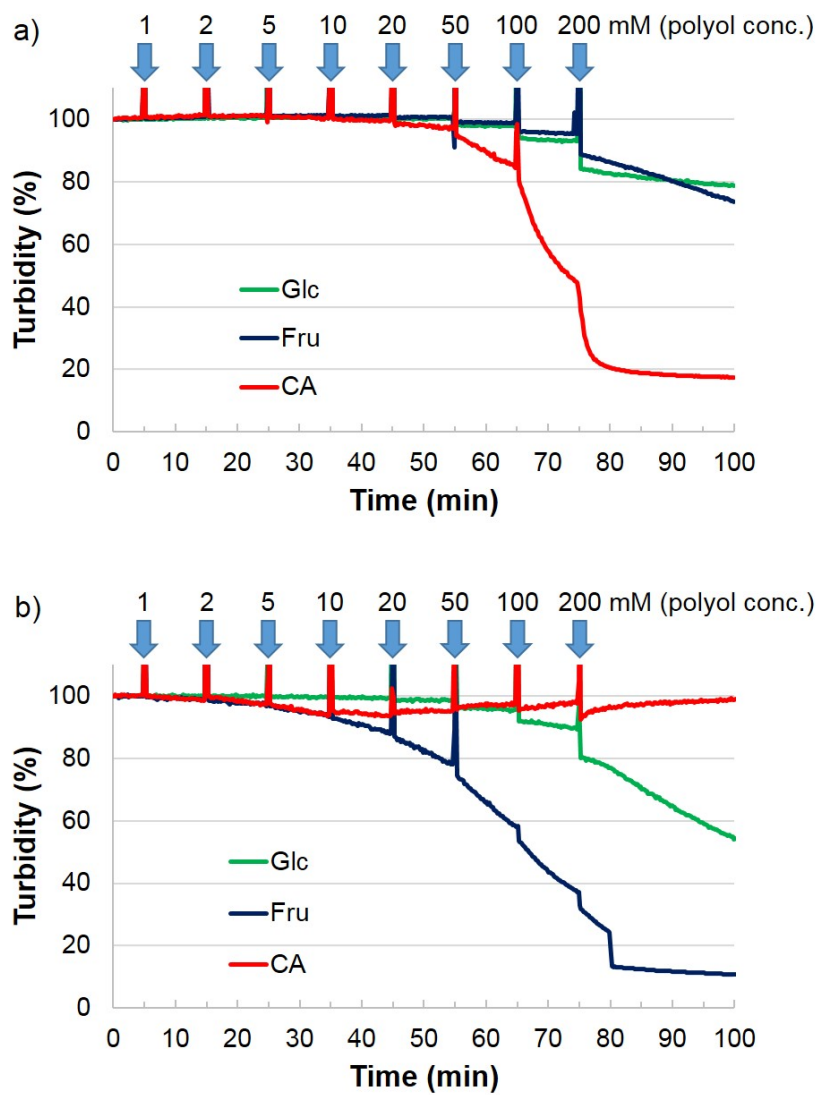


**Fig. 4** Polyol responses of the pPRXs. (a) pPRX( $\alpha$ -CyD/PBA-PEG), (b) pPRX( $\gamma$ -CyD/PBA-PEG) (pH 7.4, 37 °C)

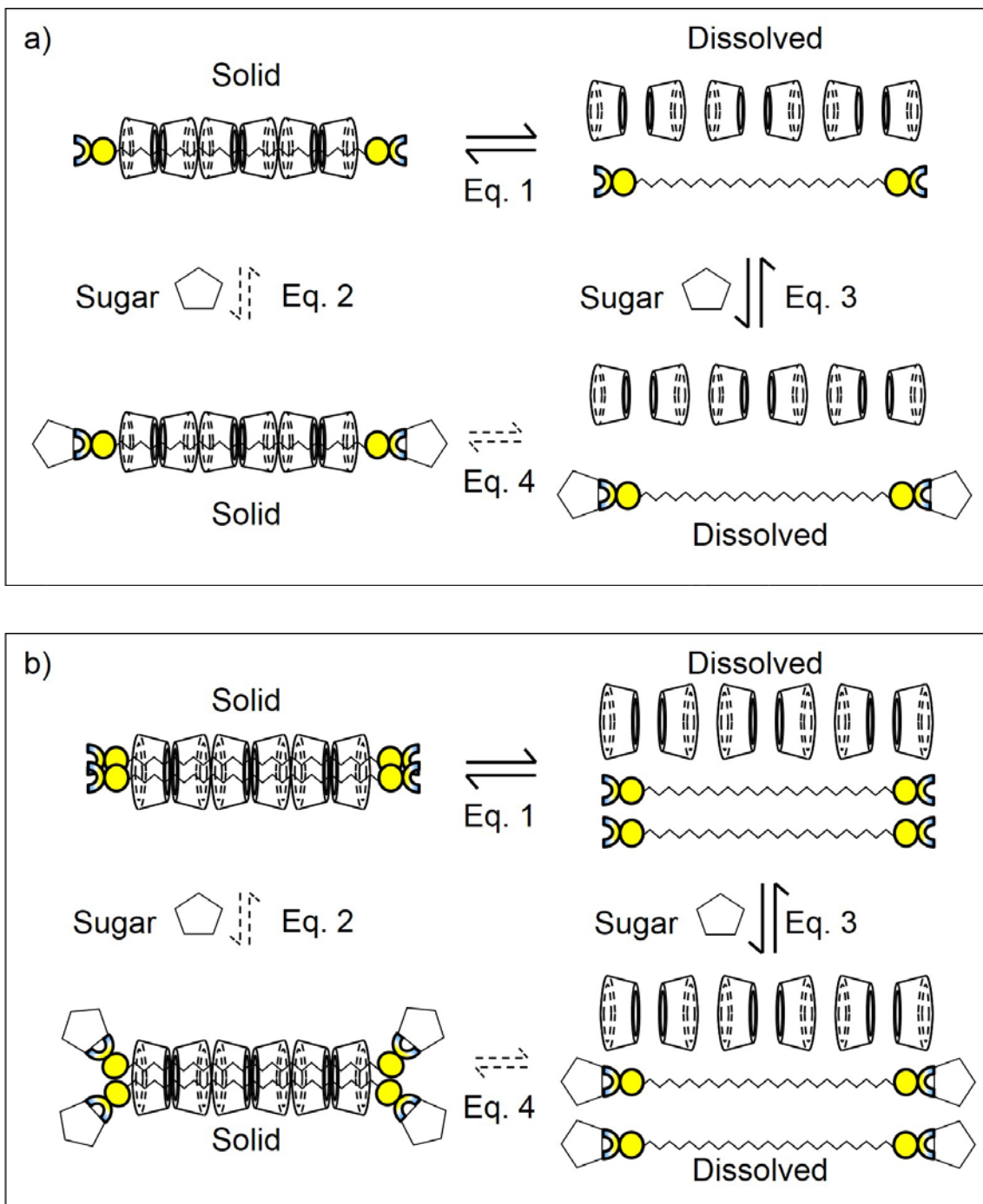


**Fig. 5** Schematics of the sugar response mechanisms of the pPRXs. (a) Sugar-induced disintegration of pPRX( $\alpha$ -CyD/PBA-PEG). (b) Sugar-induced disintegration of pPRX( $\gamma$ -CyD/PBA-PEG)

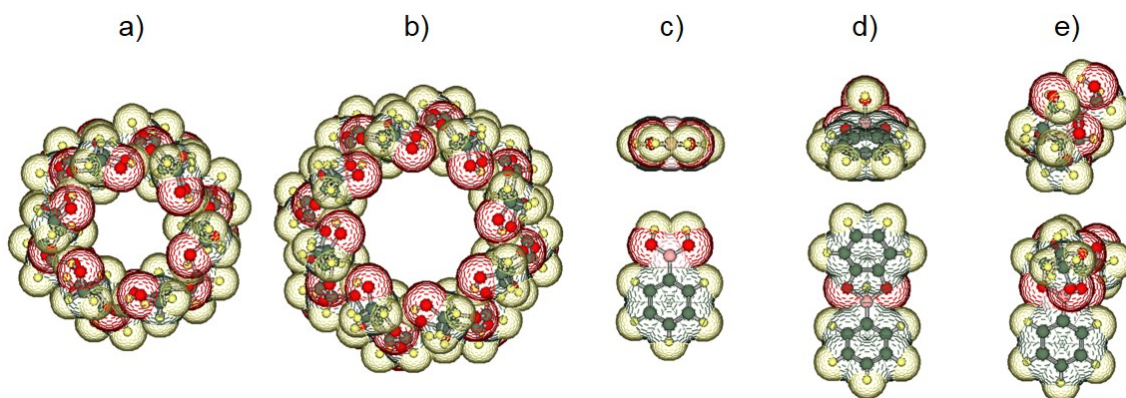


**Fig. 6** Space-filling models: (a)  $\alpha$ -CyD, (b)  $\gamma$ -CyD, (c) PBA, (d) CA-PBA, (e) Fru-PBA. (a) and (b) are based on Jmol files presented by Chaplin [37]. (c), (d), and (e) also show the figures rotated 90° around the x axis

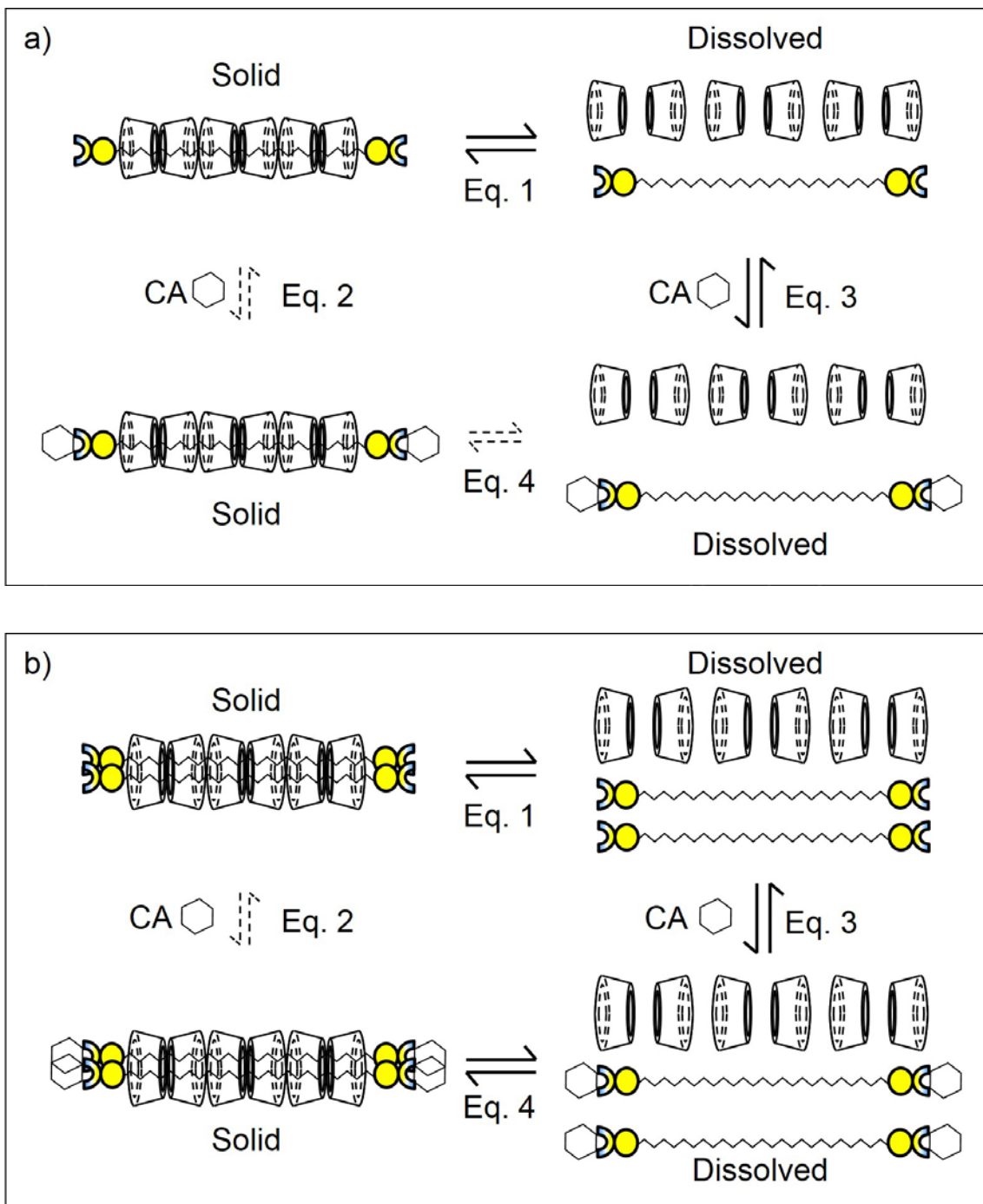


**Fig. 7** Schematics of the mechanism of CA response of the pPRXs. (a) CA-induced disintegration of pPRX( $\alpha$ -CyD/PBA-PEG). (b) CA-induced formation of pPRX( $\gamma$ -CyD/CA-PBA-PEG)

**Table 1** Crystallographic characteristics of pPRX( $\alpha$ -CyD/PBA-PEG).

$2\theta_{\text{obs}}$ (deg)	( <i>hkl</i> )	$d_{\text{obs}}$ (Å)	$d_{\text{cal}}$ (Å) <sup>a</sup>
7.48	(200)	11.81	11.81
11.88	(002)	7.44	7.44
12.90	(220)	6.86	6.82
19.80	(420)	4.48	4.46
22.56	(600)	3.94	3.94

<sup>a</sup> Calculated assuming a hexagonal unit cell with  $a = b = 27.27$  Å,  $c = 14.89$  Å.

**Table 2** Crystallographic characteristics of pPRX( $\gamma$ -CyD/PBA-PEG).

$2\theta_{\text{obs}}$ (deg)	( <i>hkl</i> )	$d_{\text{obs}}$ (Å)	$d_{\text{cal}}$ (Å) <sup>b</sup>
7.46	(200)	11.84	11.84
12.08	(002)	7.32	7.32
14.90	(400)	5.94	5.92
16.72	(420)	5.30	5.30
21.84	(530)	4.07	4.06

<sup>b</sup> Calculated assuming a tetragonal unit cell with  $a = b = 23.68$  Å,  $c = 14.64$  Å.

## Supplementary Material

### Contents

$^1\text{H}$  NMR spectra of PBA-PEG and pPRXs

The relationship between turbidity and the weight of suspended pPRX

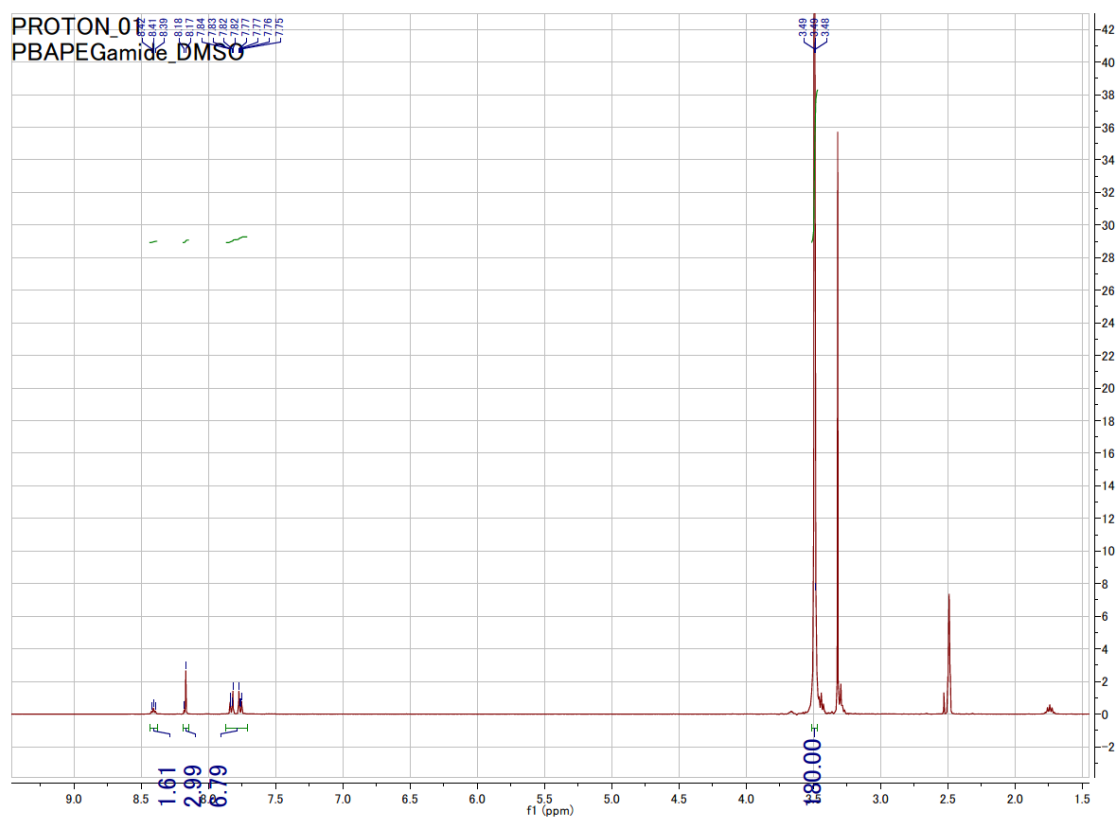


**Fig. S1**  $^1\text{H}$  NMR spectrum of PBA-PEG in  $\text{DMSO-}d_6$

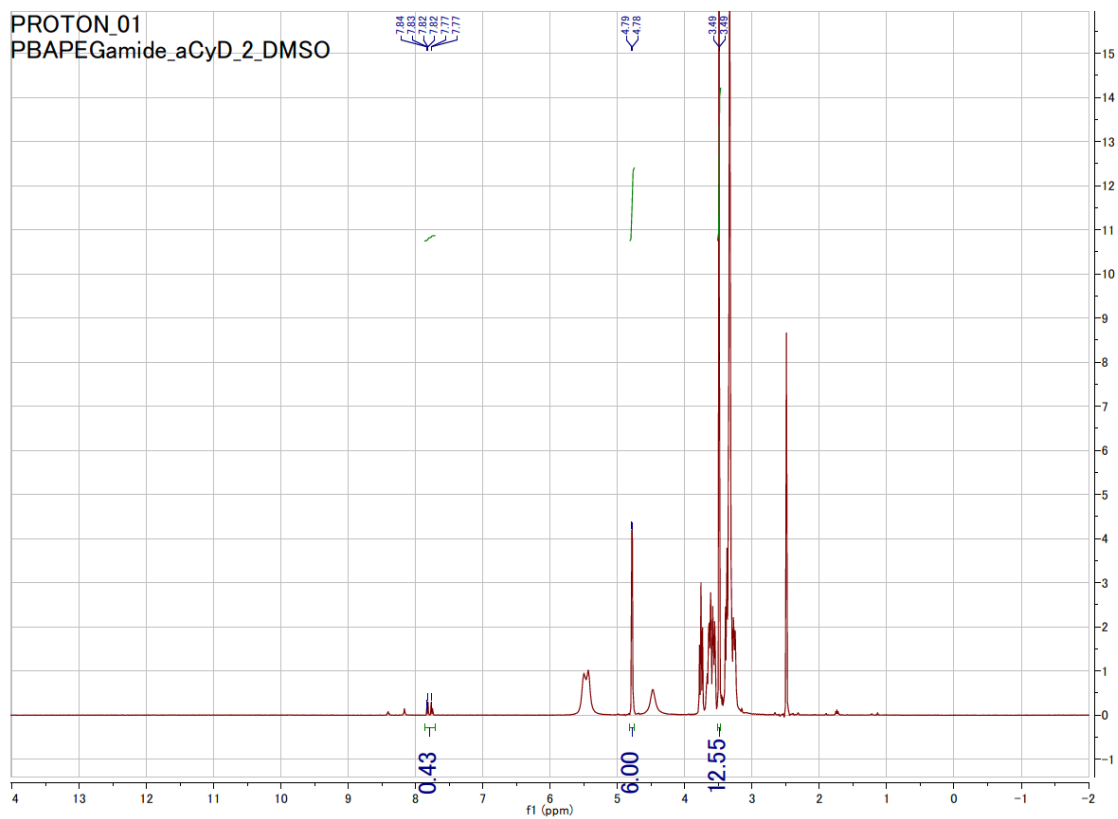


**Fig. S2**  $^1\text{H}$  NMR spectrum of components of pPRX( $\alpha$ -CyD/PBA-PEG) in  $\text{DMSO-}d_6$

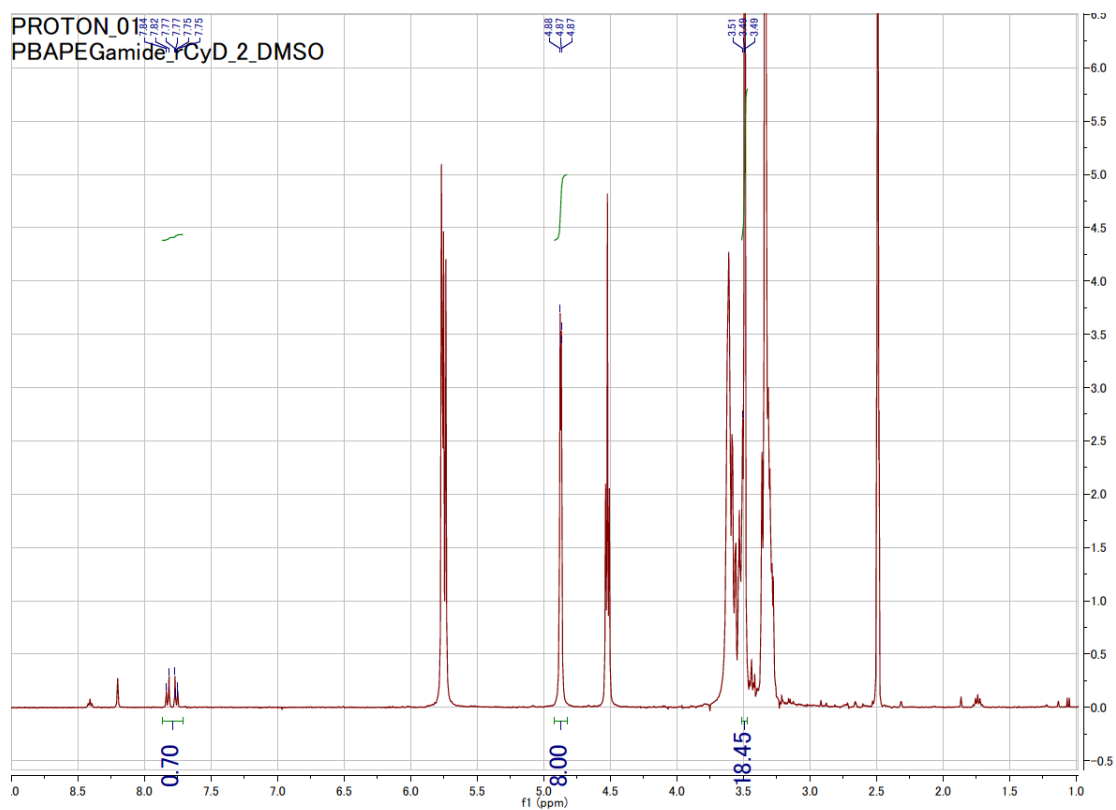


**Fig. S3**  $^1\text{H}$  NMR spectrum of components of pPRX( $\gamma$ -CyD/PBA-PEG) in  $\text{DMSO-}d_6$

### The relationship between turbidity and the weight of suspended pPRX

A buffer solution (20 mM HEPES, pH 7.4, 2.0 mL) was stirred in an absorption spectrometer cell at 37 °C. pPRX( $\gamma$ -CyD/PBA-PEG) (37 to 46 mg) was suspended in the stirred buffer solution. The turbidity was recorded by the absorbance at 700 nm. When the turbidity was allowed to reach a constant, the suspension was filtered with membrane filter, and the residue was dried to weigh the amount of solid pPRX. Fig. S4 shows the relationship between the measured absorbance value at 700 nm and the weight of the suspended particles of pPRX( $\gamma$ -CyD/PBA-PEG), which was not a simple linear relationship.

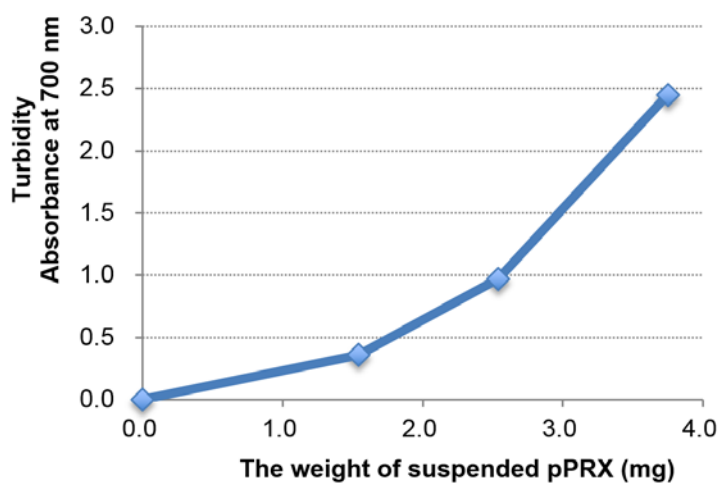


**Fig. S4** The relationship between turbidity and the weight of suspended particles of pPRX( $\gamma$ -CyD/PBA-PEG)